



Effect of nitrocarburizing and argon admixing on low carbon steel for component facility in radiometallurgical installation

Erwan HERMAWAN^{1,*}, SUPRAPTO², Usman SUDJADI¹, Siti SHALEHA¹, and Maman Kartaman AJIRIYANTO¹

¹ Center for Nuclear Fuel Research and Technology, Nuclear Energy Research Organization, National Research and Innovation Agency (BRIN), Gd. 20, Kawasan Nuklir Serpong, PUSPIPTEK, Banten 15314, Indonesia

² Center for Accelerator Research and Technology, Nuclear Energy Research Organization, National Research and Innovation Agency (BRIN), Jl. Babarsari, Daerah Istimewa Yogyakarta 55281, Indonesia

*Corresponding author e-mail: erwanhermawan29@gmail.com

Received date:

29 May 2021

Revised date:

11 October 2021

Accepted date:

28 October 2021

Keywords:

Nitrocarburizing;

Gas;

Low carbon steel

Abstract

Steel is an important component in the industrialized world with rising growth in world consumption. Steel has wide applications due to its high strength, durability, and cost-effectiveness. This has applications in the nuclear power plant. In Indonesian nuclear industry, low carbon steel is used not only for the fabrication of reactor components but also for the radiometallurgical facilities. However, to avoid the risk of premature failure and enhance the longevity of the components in the service condition, surface modification for the improvement of hardness has been realized. Amongst several methods, surface hardening by following nitrocarburizing has been found to be a successful and cost-effective method. Nitrocarburizing enable the formation of desirable phases of Fe_xN ($x = 2-3, 4$) in the compound layer and also in the diffusion layers. In the present study nitrocarburizing had been followed at variable gas ratio and temperatures. A gas mixture of 10% C_2H_2 , 50% argon, and 40% nitrogen had been fed into the reactor. The results show that there is an increase in hardness value, by addition of argon gas up to 50% in the nitrocarburizing process, making the sample harder. With the variation of temperature the enhancement of hardness could be achieved up to 7% to 10% of the initial hardness. When compared with previous studies, the maximum addition of argon is in the range of 10% to 30% because it provides a more optimal increase in hardness.

1. Introduction

Steel is an important component in the industrialized world with rising growth in the world consumption. Steel is an alloy of high strength, durability and cost-effectiveness has widespread applications in industrial sectors like; aircraft, railroad, automotive industries etc. [1,2]. In addition, steel material is also used as a construction material in the nuclear industry, including components for the Nuclear Power Plant (NPP). In Indonesian nuclear industry, steel is used in the research activities which involve hotcell components such as chains on conveyers, incell cranes and other supporting equipment that uses supporting equipment made up of low carbon steel as the base material. [3]. Steel has been the subject of research attention due to its widespread applications in various industrial sectors. However, its longevity in the service condition has been the subject of concern which leads to the surface modification. Hence, nitrocarburizing, a cost effective and successful method, has been adopted for modifying the surface in the present study.

The process involves the thermochemical diffusion of nitrogen and carbon gases at certain proportion and temperature which modifies the surface leading to enhancement of fatigue, wear and corrosion resistance. Following nitrocarburizing, a hard surface layer consisting

of a compound and diffusion layer is formed. Nitrogen and carbon enriched iron crystal lattice along with the hardened layer consisting of $\epsilon-Fe_{2-3}(N, C)_{1-z}$ and $\gamma-Fe_4N_{1-x}$ [4,5] is formed after nitrocarburizing. Previously, several studies had been carried out on nitrocarburizing by varying the process parameters temperature, time and gas concentration. Formation of these phases and the nitrogen solid solution synergistically improve the hardness and corrosion resistance of the steel. X-ray diffraction (XRD) analysis reveals the formation of γ_N and γ_C phases which had also been observed in the scanning electron microscope (SEM) analysis.

The present study was focused on a novel surface treatment of the steel which includes the variation of gas composition and the temperature. Previously, it was reported that by using only the argon gas in the process the material performance could not be achieved to the desirable level [21]. Hence, the addition of H_2 to the Ar gas to form of N_2 and H_2 gas mixture was followed with the view to enhance the properties of the steel to the desirable level. This may enhance the property of materials used for the support facilities in the hotcell so that its service life can be prolonged. On the other hand, an attempt has also been made in this study to understand the mechanics of the nitrocarburizing process.

2. Experimental

The material used in this study is low carbon steel with a carbon composition generally below 0.3% [22,23]. The composition of the steel is represented in the Table 1:

Table 1. Chemical composition of the sample.

Elements	Concentration (%)
C	0.298
Si	0.18
Mn	0.568
P	0.009
S	0.013
Cu	0.007
Al	0.002
Cr	0.009
Mo	<0.002
Ni	<0.002
V	<0.002
Ti	<0.002
Nb	<0.002
W	<0.002

The low carbon steel is used for the existing facilities in the radiometallurgical facility, Center for Nuclear Fuel Technology, especially for hot cell facilities (Figure 1). Steel samples of dimension

were cut into the area $1 \times 1 \text{ cm}^2$ with the thickness 5 mm. The surfaces were subjected to metallographic polishing by using various grades #80, #120, #500, #800, #1200, # 2400 and finally polished to a level of surface roughness to $3 \mu\text{m}$. The polished sample was cleaned using soap and ultrasonic instrument before running the nitrocarburizing process.

2.1 Nitrocarburizing process

The nitrocarburizing process uses a nitriding engine (Figure 2) made by the Center for Accelerator Science and Technology (PSTA-BATAN) which has been used for research activities on surface hardening [20,24,25]. Figure 2 shows the glow discharge plasma nitriding system

In this study, the variables used were temperature and diffused gas content. Table 2 show the variables and parameters used in the study from three parameters, the gas concentration used was 50% Argon, 10% C_2H_2 and 40% Nitrogen. The time used is constant for 6 h. The voltage is adjusted from 300 V to 400 V to obtain different temperatures which are 300°C and 400°C . After carrying out the nitrocarburizing process, an XRD test was carried out with an angle of 20° to 80° which use cobalt as source (Empyrean XRD). The scan rate used as 0.02° per second. The sample was cut to obtain a cross section image and then mounted for the SEM process. The sample was etched using a 2% nital solution on to see the grain boundaries of the layer. After that, the microhardness testing was carried out by using load 50 g.

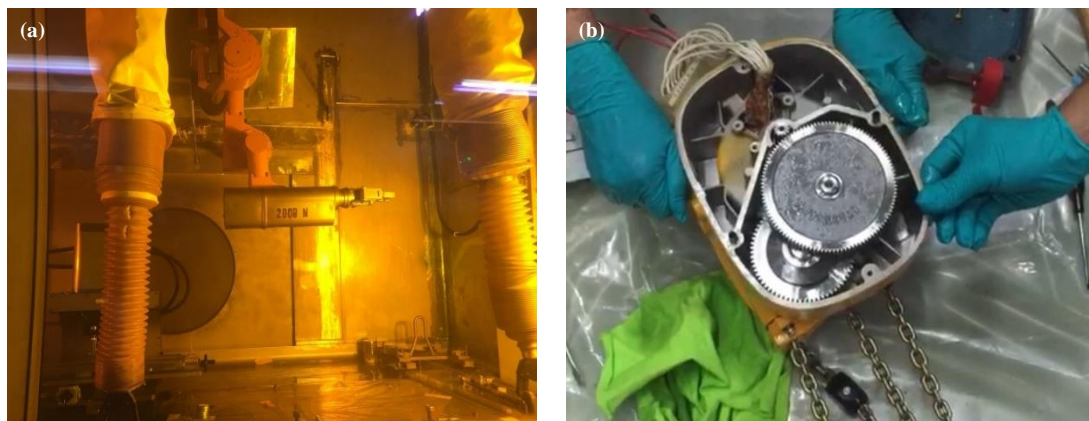


Figure 1. (a) Facilities inside the hot cell, and (b) components inside of the crane.

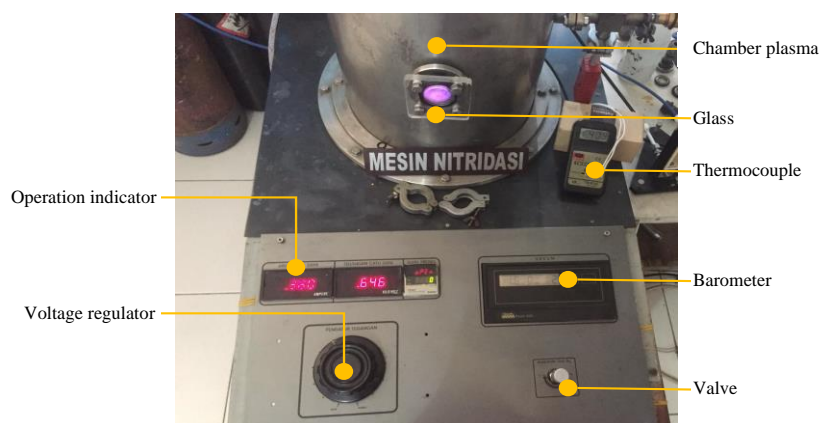


Figure 2. DC-plasma glow discharge nitriding system installation at the Center for Accelerator Science and Technology (PSTA-BATAN).

Table 2. Variables and parameters used.

Sample	Time (h)	Gas ratio	Temperature (°C)
Low Carbon Steel raw material (LCS 1)	-	-	-
Low Carbon Steel 2 (LCS 2)	6	50% Argon (Ar), 10% C ₂ H ₂ , 40% Nitrogen (N)	300
Low Carbon Steel 3 (LCS 3)	6	50% Argon (Ar), 10% C ₂ H ₂ , 40% Nitrogen (N)	400

3. Result and discussion

From this research several test results were obtained, tests carried out to determine the characteristics of the material after the nitrocarburizing process was carried out. The following are the results of the tests that have been carried out:

3.1 Hardness test result

Hardness test is carried out using the Vickers method. The hardness test results show that there is an increase in the surface hardness of the material. The untreated sample was LCS 1 which had a hardness value of 192 Hv. After the nitrocarburizing process was carried out for 6 h at a temperature of 300°C, the hardness value increased by 7% to 206 HV, while using a temperature of 400°C the hardness value was 233 Hv, or an increase of 20% from the initial hardness value. When compared with previous studies [20], by using argon content 10% to 30%, the maximum hardness was obtained with argon content of 10% with a maximum hardness value of 214 Hv. In this study, a higher hardness value was obtained due to the difference in time used when compared to previous studies. In certain conditions the surface hardness of the material is more optimal than if argon is not used because argon can increase the dissociation process and ion density on the metal surface, even the use of more than 70% argon can further increase the dissociation rate of ions that diffuse onto the metal surface [21,26]. The use of nitrogen without being associated with other gases will find it difficult to achieve a high dissociation rate, because nitrogen has a fairly high stable binding energy. In order to increase the dissociation rate, other gases such as argon or hydrogen can be used [27,28].

Cross sectional hardness measurements had shown that the hardness decreases with the depth from the surface towards the bulk as represented in Figure 4. The farther away from the surface indicates a decrease in the value of hardness. At a distance of 0.1 mm away from the surface all the steel samples had shown a decrease in hardness. Hardness at a distance of 0.1 mm away from the surface was found to be 183.81 Hv, and at 1.00 mm distance reduced to 162.05 Hv. Likewise, the nitrocarburizing treatment at 400°C from 214.75 Hv to 177.96 Hv the diffusion process does not reach the center of the sample substrate.

3.2 X-ray diffraction characterization

From the XRD data, the expanded layer was indicated by a diffraction pattern in some angles. Figure 5 shows the results of XRD testing where the most intense peak is the substrate (Fe). The XRD pattern of the steel not prominent to reveal the phase formed after nitrocarburizing at 300°C may be because the intensity of this peak is suppressed by the presence of the intense peak of the substrate. It may due to the intensity of the substrate peak is significantly high or it may be stated as the volume fraction of the formed phase is very small [16].

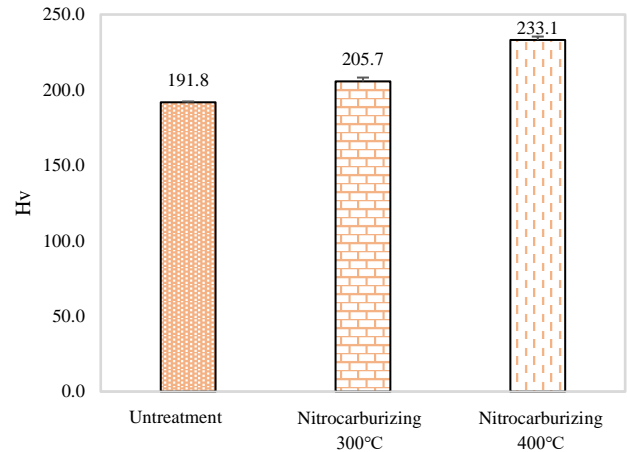


Figure 3. Representation of hardness of steel before and after nitrocarburizing at 300°C and 400°C.

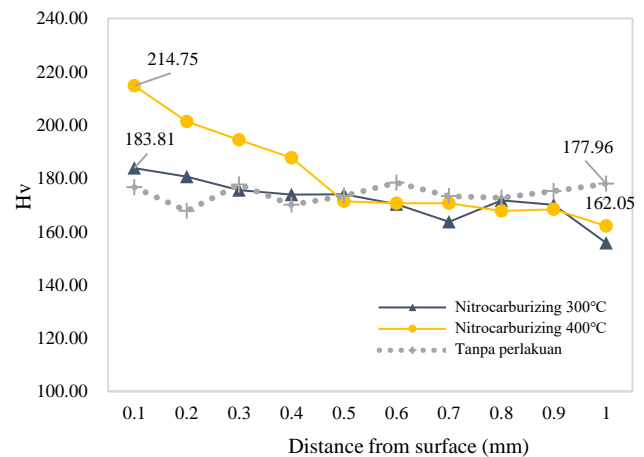


Figure 4. Hardness vs. depth profile of the cross section of steels after nitrocarburizing at various treatment conditions.

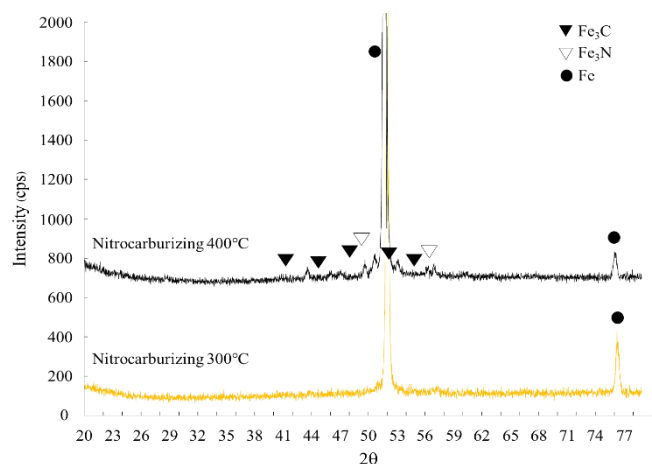


Figure 5. XRD patterns of the steel after nitrocarburizing at 300°C and 400°C.

With the increasing temperature of the nitrocarburizing process, several peaks can be seen indicating the formation of a thin compound layer. Figure 5 shows that the XRD test results show that several new phases were formed, namely Fe_3C and Fe_3N . The reflection for the Fe_3C phase appeared at 2θ diffraction angles 44° , 46.53° , 47.58° , 50.18° , 53.59° , and 56.75° . While the Fe_3N reflection phase is at an angle of 2θ 51.29° and 57.63° .

In the results of this nitrocarburizing process, diffusion of N is dominant as compared to that of C. It is because of the diffusion coefficient of C is more than that of N. This is because depends on the reaction on the surface. The C atom has a lower solubility level than the N atom, so that the C atom is formed earlier than the N atom. This can be seen in the graph between the concentration between the C and N atoms on the surface [4,29]. Figure 6 shows the process of phase formation on the surface of the material. Based on previous research [29,30,31] that the initial phase of the nitrocarburizing process is Fe_3C . The iron-carbonitride $\epsilon\text{-Fe}_2(\text{N}, \text{C})$ 1-z phase can be formed if it is carried out in a high nitrocarburizing process. So that the XRD results are dominated by Fe_3C phase atoms compared to Fe_3N and are still in the early stages of phase formation.

3.3 Scanning electron microscopy (SEM) characterization

From Figure 7 and Figure 8 it can be seen that there is a thin expanded layer on the surface of the material both in the 300°C and 400°C nitrocarburizing processes, which marked by darker colored layer. In the picture on the left side is a cross section microstructure with a magnification of $240\times$. In bottom part of image shows the SEM results with a magnification of $5000\times$, so it can be seen a thin ϵ layer on the surface. In the 300°C nitrocarburizing process, an expanded layer or compound zone was obtained [32] $5.2\ \mu\text{m}$ to $5.7\ \mu\text{m}$, while for the 400°C nitrocarburizing process, a thicker thickness was obtained, which is $4.45\ \mu\text{m}$ to $6.2\ \mu\text{m}$, where in this part of the layer has the maximum hardness value. In Figure 8 it is also clearly seen the compound layer. In the part which marked by white box are diffusion zone, but from microstructure or SEM imaging the diffusion zone is not appear [32]. In Figure 7 and Figure 8, there are cavities and irregular surfaces on the surface, this is because the role of argon is not only to accelerate the reaction process but also to cause damage to the metal surface due to the collision process between ions that occurs on the surface so that the surface defects are increasing [33].

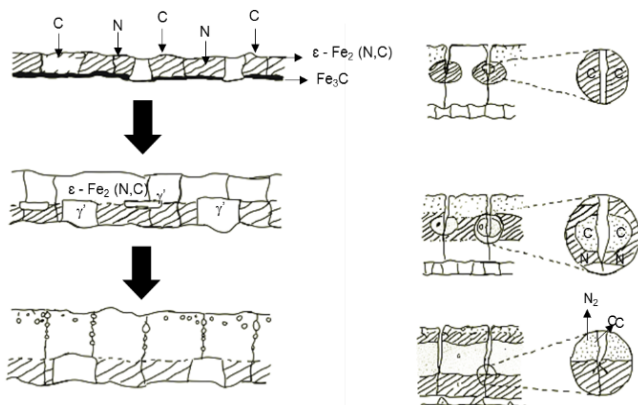


Figure 6. Layers growth process of C and N [30].

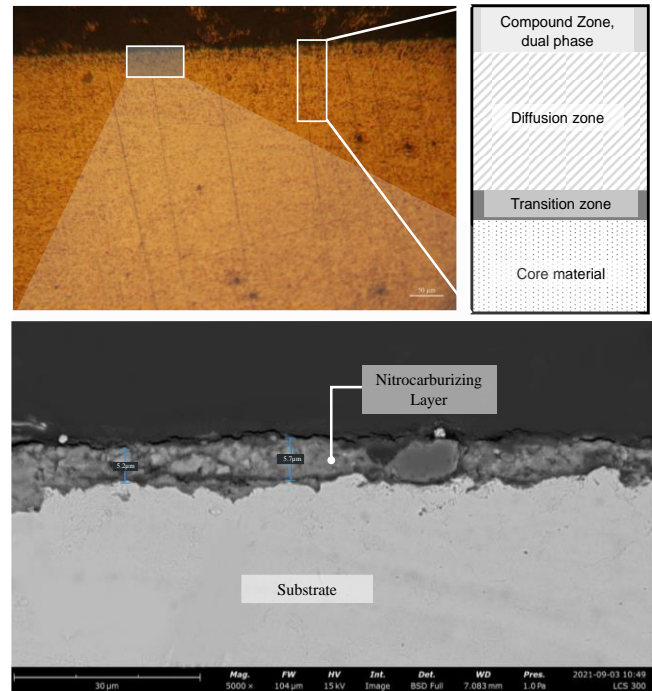


Figure 7. SEM characterization on cross-sectional after nitrocarburizing at 300°C .

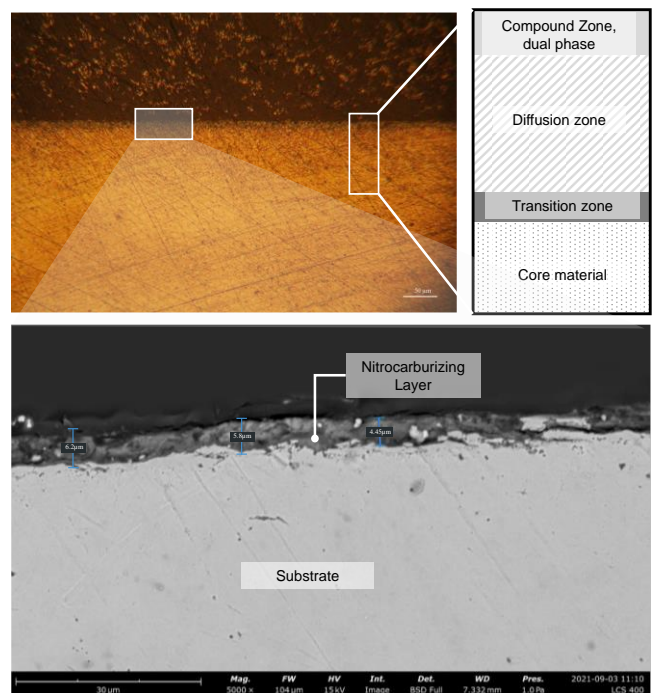


Figure 8. SEM characterization on cross-sectional after nitrocarburizing at 400°C .

From the Figure 9 and Figure 10, the Energy-dispersive X-ray spectroscopy (EDS) was conducted by using map and line features. Based on Figure 9(a), from the EDS mapping shows that in red colour is carbon diffusion, while the blue colour is Fe zone. If the line feature used from A to B (Figure 9(b) and Figure 10(b)) along $8\ \mu\text{m}$, it can be seen the carbon percentage from the surface is decrease at $1\ \mu\text{m}$ of depth, but the there is an increase in carbon concentration at $1\ \mu\text{m}$ to $5\ \mu\text{m}$ of depth. This condition is also obtained at 400°C nitrocarburizing process (Figure 10(b)). This phenomenon also obtained

from previous research [34,35], the low amount of nitrogen concentration due to the thermodynamic stability of nitrides in relation to the carbide. The high solubility of nitrogen pushes carbon atoms towards the interior of the steel, thus forming a carbon layer at the boundary area between the substrate and the expanded layer [36,37]. From map and line feature is not clearly seen the nitrogen concentration, it is because to obtain nitrogen with high concentration need higher temperature and nitrogen gas ratio. While based on kinetic of compound layer growth this result categorize as first stage, where in this stage characterised by relatively slow layer growth kinetics [38,39]. In this experiment the nitrocarburizing obtained under 500°C due to the old plasma nitrocarburizing tools which can not reach maximum temperature process and optimum hardness value, based on literature best temperature use for nitrocarburizing at range 525°C to 625°C and the hardness value at range 300 H_v to 1200 H_v [40,41].

Based on quantitative analysis from EDS both specimens which process at 300°C and 400°C (Figure 11 (a) and (b)) have similar characteristic. It can be found C, Fe, and small energy intensity of N atom peak.

In Figure 12, the C atom is higher at 300°C nitrocarburizing process with total concentration of 18.1% and 17.1% at 400°C nitrocarburizing process. Otherwise the N atom increase from 0.4% to 3.8% at 400°C nitrocarburizing process. The N atom concentration increase because of different nitrocarburizing temperature. Based on previous discussion that the N atom concentration will also rise if used higher temperature process.

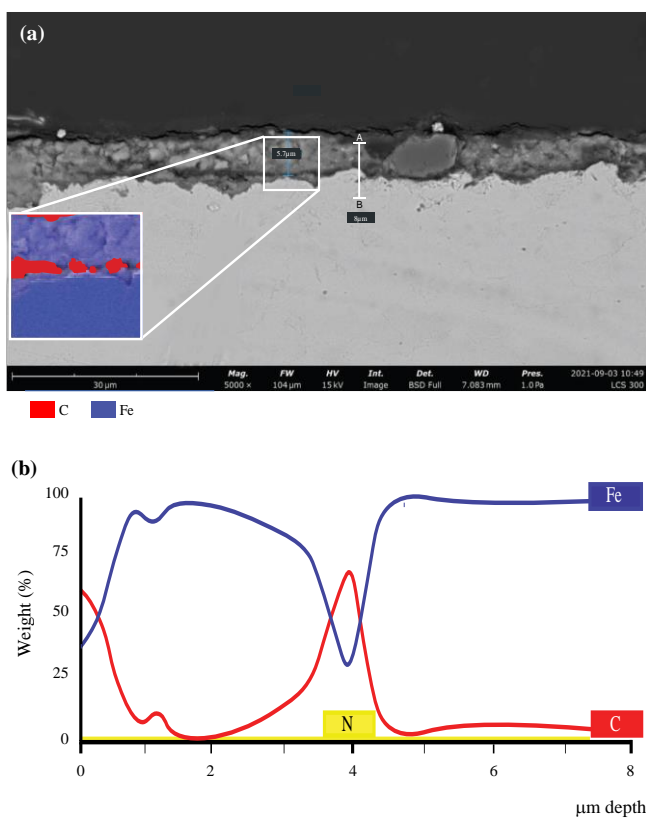


Figure 9. (a) Element mapping analysis at 300°C nitrocarburizing process, (b) C, N, and Fe concentration based on line analysis at 300°C nitrocarburizing process.

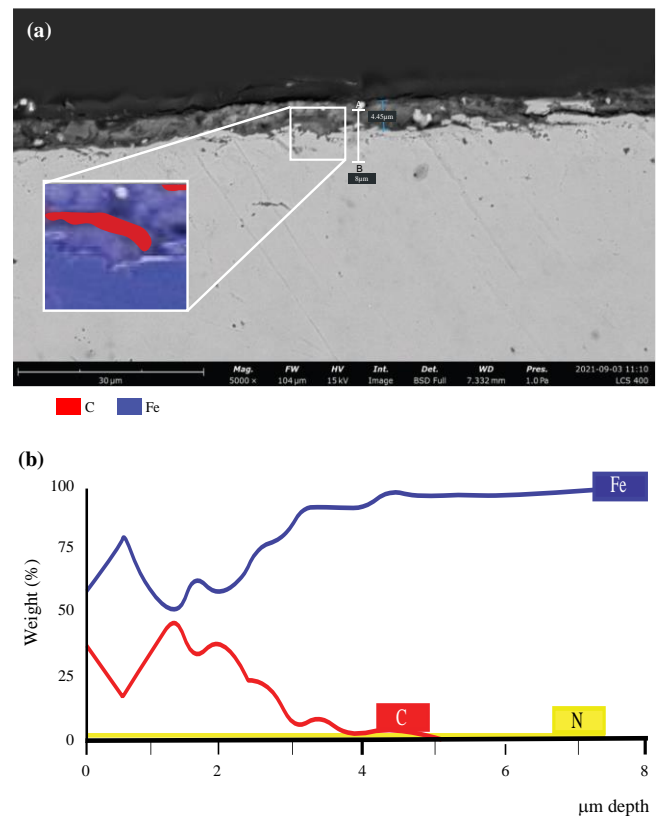


Figure 10. (a) Element mapping analysis at 400°C nitrocarburizing process, (b) C, N, and Fe concentration based on line analysis at 400°C nitrocarburizing process.

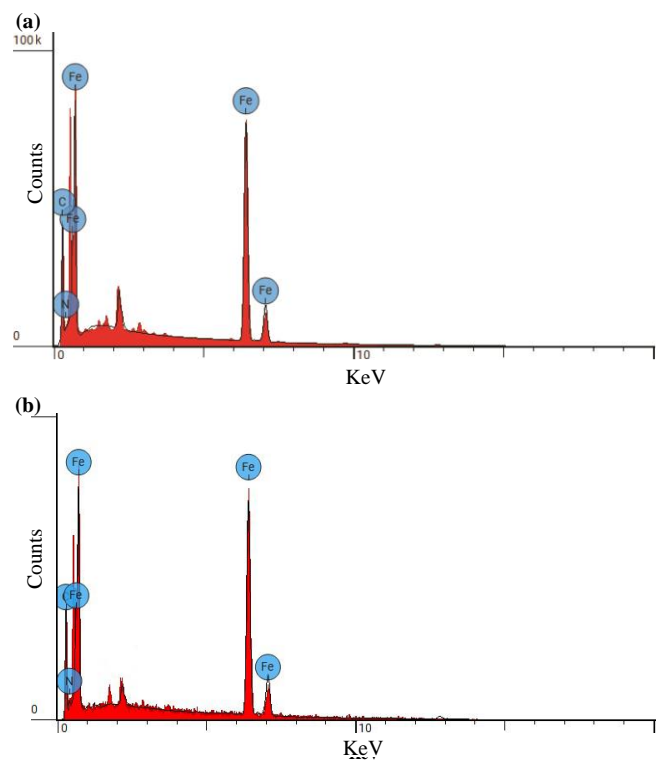


Figure 11. Quantitative analysis from EDS mapping (a) at 300°C nitrocarburizing process (b) at 400°C nitrocarburizing process.

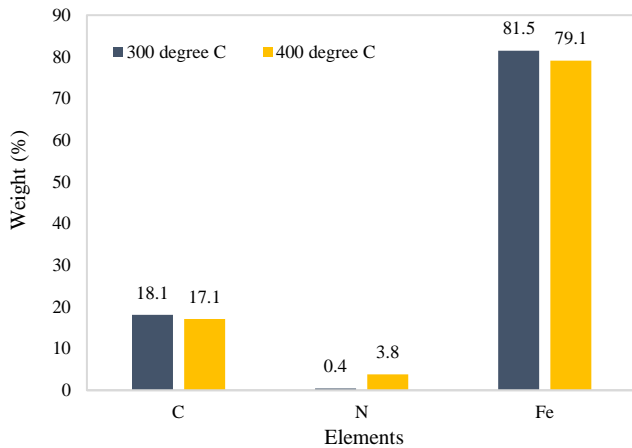


Figure 12. Concentrations of C, N, and Fe from mapping analysis at different variable nitrocarburizing process.

4. Conclusion

Based on the results of the study, the hardness value was obtained by performing surface hardening on the low carbon steel surface. The addition of argon gas up to 50% in the nitrocarburizing process generate the harder specimen. The hardness was obtained based on the difference in temperature which made an increase of 7% to 20% from the initial hardness value. When compared with previous studies, the maximum addition of argon is in the range of 10% to 30% because it provides a more optimal hardness value. Based on the results of XRD analysis, the increase in hardness is due to a new phase formed on the surface of the material, which are Fe_3C and Fe_3N phases. These phases form a compound layer after being observed using SEM and EDS analysis.

Acknowledgements

We thank to Mr. Cipto (Center for Science and Accelerator Technology) for the advise and knowledge, Mrs. Deswita (Center for Science and Advanced Material Technology) for helping in SEM data acquisition, Mr. Slamet (Center for Nuclear Fuel Technology), and many else who couldn't we described.

References

- [1] World Steel Association, *2020 World Steel in Figures*, 2020, p 7.
- [2] S. N. Abdullah, N. Sazali, and A.S. Jamaludin, "Study of low carbon steel in rapid cooling process: A short review," *Journal of Modern Manufacturing Systems and Technology*, vol. 4, pp. 52-59, 2020.
- [3] Sungkono, M. K. Ajiriyanto, S. Ismawanti, and R. Sigit, "characterization of microstructure, hardness, chemical composition and crystal structure of layers on steel surface," *Urania*, vol. 25, no. 3, pp 141-204, 2019.
- [4] M. A. J. Somers, "Nitriding and nitrocarburizing; current status and future challenges," *Paper presented at Heat Treat & Surface Engineering Conference & Expo 2013*, Chennai, India.
- [5] M. J. Schneider, and M. S. Chatterjee, "Introduction to surface hardening of steels," *ASM Handbook*, vol. 4A, pp. 389-398, 2013.
- [6] P. Cisquini, S. V. Ramos, P. R. P. Viana, V. de Freitas Cunha Lins, A. R. Franco, and E. A. Vieira, "Effect of the roughness produced by plasma nitrocarburizing on corrosion resistance Of AISI 304 austenitic stainless steel," *Journal of Surface & Coatings Technology*, vol. 204, pp. 3004-3008, 2019.
- [7] D. dos Santos Filho, A. P. Tschiptschin, and H. Goldenstein, "Effects of shallow plasma nitriding on the surface topography of gray cast iron specimens," *Surface & Coatings Technology*, vol. 404, p. 126464, 2019.
- [8] K. R. M. Rao, C. Nouveau, and K. Trinadh, "Effects on corrosion resistance of low alloy steel after plasma nitriding at elevated temperature," *Materials Today Proceedings*, vol. 17, pp. 26-33, 2019.
- [9] S. M. Jafarpour, A. Puth, A. Dalke, J. Bocker, A. Pipa, J. Ropcke, J.-P. H. V. Helden, and H. Biermann, "Solid carbon active screen plasma nitrocarburizing of AISI 316L stainless steel in cold wall reactor: Influence of plasma conditions". *Material Research and Technology*. vol. 9. no. 4, pp. 9195-9205, 2020.
- [10] L. Tang, C. Mao, W. Jia, K. Wei, and J. Hu, "The effect of novel composite pretreatment on performances of plasma nitrided layer," *Material Research and Technology*, vol. 9, no. 5, pp. 9531-9536, 2020.
- [11] C. E. Foerster, A. Assmann, S. L. R. D. Silva, and F. C. N. Borges, "AISI 304 nitrocarburized at low temperature: Mechanical and tribological properties," *Surface & Coatings Technology*, vol. 204, pp. 3004-3008, 2010.
- [12] R. Huang, J. Wang, S. Zhong, M. Li, J. Xiong, and H. Fan, "Surface modification of 2205 duplex stainless steel by low temperature salt bath nitrocarburizing at 430°C," *Applied Surface Science*, vol. 271, pp. 93-97, 2013.
- [13] A. D. Anjos, C. J. Scheuer, S. F. Brunatto, and R. P. Cardoso, "Low-temperature plasma nitrocarburizing of the AISI 420 martensitic stainless steel: Microstructure and process kinetics," *Surface & Coatings Technology*, vol. 275, pp. 51-57, 2015.
- [14] H. Shen, and L. Wang, "Mechanism and properties of plasma nitriding AISI 420 stainless steel at low temperature and anodic (ground) potential," *Surface & Coatings Technology*, vol. 403, p. 126390, 2020.
- [15] M. K. Zarchi, M. H. Shariat, S. A. Dehghan, and S. Solhjoo, "Characterization of nitrocarburized surface layer on AISI 1020 steel by electrolytic plasma processing in an urea electrolyte," *Materials Research and Technology*, vol. 2. no. 3, pp. 213-220, 2013.
- [16] Y.-W. Cho, Y.-J. Kang, J.-H. Baek, J.-H. Woo, and Y.-R. Cho, "Investigation of microstructure, nanohardness and corrosion resistance for oxi-nitrocarburized low carbon steel," *Metals*, vol. 9, pp. 190, 2019.
- [17] F. A. P. Fernandes, L. C. Casteletti, and J. Gallego. "Microstructure of nitrided and nitrocarburized layers produced on a superaustenitic stainless steel," *Materials Research and Technology*, vol. 2, no. 2, pp. 158-164, 2013.
- [18] J. Z. L. Lu, W. N. Zhou, W. H. Zang, and K. Shiozawa, "Effects of nitrocarburizing on fatigue property of medium carbon steel

- in very high cycle regime,” *Materials Science and Engineering*, vol. 528, pp. 7060-7067, 2011.
- [19] I. Lee, “Combination of plasma nitriding and nitrocarburizing treatments of AISI 630 martensitic precipitation hardening stainless steel,” *Surface & Coatings Technology*, vol. 376, pp. 8-14, 2019.
- [20] Suprpto, T. Sujitno, W. Andriyanti, I. Aziz, E. M. Saefurrohman, and A. Anggraini, “Effect of post treatment and addition of argon gas on the properties of plasma nitrocarburized local disc brake materials,” in *AIP Conference Proceedings*, vol. 2296, p. 20085, 2020.
- [21] M. Naeem, J. Iqbal, M. Abrar, and K. H. Khan, “The effect of argon admixing on nitriding of plain carbon steel in N₂ and N₂-H₂ plasma,” *Surface & Coatings Technology*, vol. 350, pp. 48-56, 2018.
- [22] T. Islam, and H. M. M. A. Rashed, “Classification and application of plain carbon steels” in *Materials Science and Materials Engineering*, Elsevier, 2019
- [23] R. Singh, “Classification of steels,” in *Applied Welding Engineering*, R. Singh, Eds., 3rd ed., Butterworth Heinemann: Oxford, UK, 2020, pp. 53-60.
- [24] S. Suprpto, T. Sujitno, P. Aziz, and W. Andriyanti, “Effect of post treatment in argon environment of plasma nitrided local disc brake,” *Advanced in Materials*, vol. 8, no. 1, pp. 27-32, 2019.
- [25] U. Sudjadi, “Study about surface hardening on local disc brakes with direct current plasma nitrocarburizing apparatus,” *Advanced Materials Research*, vol. 789, pp. 383-386, 2013.
- [26] P. G. Reses, E. Mendez, D. Osorio-Gonzalez, F. Castillo, and H. Martinez, “Electron temperature and ion density measurements in a glow discharge of an Ar–N₂ mixture,” *Radiation Effects & Defects in Solids*, vol. 169, No. 4, pp. 285-292, 2014.
- [27] N. U. Rehman, Z. Anjum, A. Masood, M. Farooq, I. Ahmad, and M. Zakaullah, “Metrology of non-thermal capacitively coupled N₂–Ar mixture plasma,” *Optics Communications*, vol. 296, pp. 72-78, 2013.
- [28] M. Tabbal, M. Kazpoulo, T. Chritidis, and S. Isber, “Enhancement of the molecular nitrogen dissociation levels by argon dilution in surfacewave-sustained plasmas,” *Applied Physics Letters*, vol. 78, no. 15, p. 2131, 2001.
- [29] M. A. J. Somers, “Heat treatment and surface engineering in the twenty-first century,” *International Heat Treatment and Surface Engineering*, vol. 5, pp. 5-16, 2011.
- [30] M. A. J. Somers, and E. J. Mittemeijer, “Verbindungsschichtbildung während des Gasnitrierens und des Gas- und Salzbadnitrocarburierens,” *Heat Treatment and Materials* vol. 47, pp. 5-13. 1992.
- [31] T. Woehrl, A. Leineweber, and E. J. Mittemeijer. “Microstructural and phase evolution of compound layers growing on α -iron during gaseous nitrocarburizing,” *Metallurgical and Materials Transactions A*, vol. 43, no. 7, pp. 2401-2413, 2012
- [32] D. Pye, “Practical nitriding and ferritic nitrocarburizing,” ASM International Materials Park, Ohio, USA, pp. 31-32, 2003.
- [33] A. H. Razemani, A. H. Sari, and Ali Shokouhy. “The effects of argon ion bombardment on the corrosion resistance of tantalum,” *International Nano Letters*, vol. 7, no. 1, pp. 51-57, 2021.
- [34] T. Christiansen, and M. A. J. Somers, “Low-temperature surface hardening of stainless steel,” *Advanced Materials and Process*, vol. 52, pp. 16-17. 2013.
- [35] M. A. Fontes, V. H. B. Scheid, D. de Souza Machado, L. C. Casteletti, and P. A. de Paula Nascente, “Morphology of the DIN 100Cr6 Case hardened steel after plasma nitrocarburizing process,” *Material Research*, vol. 22, pp. 1-6, 2019.
- [36] E. J. Mittemeijer, “Fundamentals of nitriding and nitrocarburizing”. In: Dossett J, Totten GE, eds. *ASM Handbook*, vol. 4A: Steel Heat Treating Fundamentals and Processes. Materials Park: ASM International, 2013
- [37] I. Lee, “Effect of processing temperatures on characteristics of surface layers of low temperature plasma nitrocarburized AISi 204 Cu austenitic stainless steel”. *Transactions of Nonferrous Metals Society of China*, vol. 22, pp. 678-682, 2012.
- [38] M. A. J. Somers, and E. J. Mittemeijer, “Formation and growth of compound layer on nitrocarburizing iron: kinetics and microstructural evolution,” *Surface Engineering*, vol. 3, no. 2, pp. 123-137, 1987.
- [39] M. A. J. Somers, and E. J. Mittemeijer, “Layer-growth kinetics on gaseous nitriding of pure iron: evaluation of diffusion coefficient for nitrogen in iron nitride,” *Metallurgical and Material Transactions*, vol. 26A, pp. 57-74, 1995.
- [40] D. Pye, “Nitriding and Nitrocarburizing”. *Encyclopedia of Tribology*, pp. 2421-2428, 2013.
- [41] M. Reger, R. Horvath, A. Szell, T. Reti, V. Gonda, and Imre Felde, “The relationship between surface and in-depth hardness for the nitrocarburizing treatment process,” *Metal*, vol. 11, pp. 1-15. 2021.